Atmos. Chem. Phys. Discuss., https://doi.org/10.5194/acp-2018-247
Manuscript under review for journal Atmos. Chem. Phys.
Discussion started: 25 April 2018

Atmospheric Chemistry and Physics
Discussions

The evaluating study of the momentum and heat exchange process of two surface layer schemes during the severe haze pollution in east China

Yue Peng[1,2], Hong Wang[1,2], Yubin Li[3], Changwei Liu[3], Tianliang Zhao[2], Xiaoye Zhang[1], Zhiqiu Gao[3,4], Huizheng Che[1], Meng Zhang[5]

[1] State Key Laboratory of Severe Weather/Institute of Atmospheric Composition, Chinese Academy of Meteorological Sciences (CMAS), Beijing 100081, China

[2] Collaborative Innovation Center on Forecast and Evaluation of Meteorological Disasters/Key Laboratory for Aerosol-Cloud-Precipitation of China Meteorological Administration, Nanjing University of Information Science and Technology, Nanjing 210044, China

[3] Key Laboratory of Meteorological Disaster of Ministry of Education/Collaborative Innovation Center on Forecast and Evaluation of Meteorological Disasters, School of Remote Sensing and Geomatics Engineering, Nanjing University of Information Science and Technology, Nanjing 210044, China

[4] State Key Laboratory of Atmospheric Boundary Layer Physics and Atmospheric Chemistry, Institute of Atmospheric Physics, Chinese Academy of Sciences, Beijing 100029, China

[5] Beijing Meteorological Service, Beijing 100089, China

Correspondence to: Hong Wang (wangh@cma.gov.cn)

Abstract. The turbulent flux parameterization schemes in surface layer are crucial for air pollution modeling. The pollutants prediction by atmosphere chemical model exist obvious deficiencies, which may be closely related to the uncertainties of the momentum and sensible heat fluxes calculation in the surface layer. In this study, a new surface layer scheme (Li) and a classic scheme (MM5) were compared and evaluated based on the observed momentum and sensible heat fluxes in east China during a severe haze episode in winter. The results showed that it is necessary to distinguish the thermal roughness length z_{0h} from the aerodynamic roughness length z_{0m}, and ignoring the difference between the two led to large errors of the momentum and sensible heat fluxes in MM5. The error of calculated sensible heat flux was reduced by 54% after discriminating z_{0h} from z_{0m} in MM5. Besides, the algorithm itself of Li scheme performed generally better than MM5 in winter in east China and the momentum flux bias of the Li scheme was lower about 12%, sensible heat flux bias about 5% than those of MM5 scheme. Most of all, the Li scheme showed a significant advantage over MM5 for the transition stage from unstable to stable atmosphere corresponding to the $PM_{2.5}$ accumulation. The momentum flux bias of Li was lower about 38%, sensible heat flux bias about 43% than those of MM5 during the $PM_{2.5}$ increasing stage. This study result indicates the ability of Li scheme for more accurate describing the regional atmosphere stratification, and suggests the potential improving possibilities of severe haze prediction in east China by online coupling it into the atmosphere chemical model.

Key words: surface layer; turbulent flux parameterization; roughness length; numerical modeling; air pollution

1 Introduction

Adequate air quality modeling relies on accurate simulations of meteorological conditions, especially in planetary boundary layer (PBL) (Hu et al., 2010; Cheng et al., 2012; Xie et al., 2012). The PBL is closely coupled to the earth's surface by turbulent exchange processes. The surface layer (SL) close to the earth's surface reflects the surface state by calculating momentum, heat, water vapor and other fluxes, and influences the atmospheric structure by turbulent transport process. The SL provides important bottom boundary conditions, as the bottom layer of the PBL. In addition, atmospheric conditions in both the PBL and upper layers are strongly dependent on the turbulent fluxes which are computed in the SL (Ban et al., 2010). Flux parameterization in the SL plays an important role in studies of the hydrological cycle and weather prediction (Yang et al., 2001; Li et al., 2014).

In many numerical models, surface momentum, heat and moisture fluxes calculated by a SL scheme are coupled to a Land Surface Module, which in turn provides input to the PBL module. Therefore, an adequate SL scheme is crucial for the model performance (Jiménez et al., 2012). It was reported that the difference of 2-m temperature modeling in three PBL schemes is due to different calculation of sensible heat fluxes in the SL (Hu et al., 2010). Tymvios et al.(2017) evaluated the perfomence of Weather Research and Forecasting (WRF) model with a combination of several PBL and compatible SL schemes and emphasized the importance of SL schemes.

Most SL schemes used in numerical models are bulk algorithms which are based on Monin-Obukhov similarity theory (hereinafter MOST, Monin and Obukhov, 1954). In a bulk algorithm, vertical fluxes in the SL can be considered constant. The effects of shear stress and buoyancy on turbulent transport are discussed with the method of similarity theory and dimensional analysis. Turbulent fluxes in models are parameterized by wind, temperature, moisture in the lowest layer, surface skin temperature and humidity. Many international scholars verified the MOST using of field experiments and then proposed the universal functions, the commonly used of which is Businger-Dyer (BD) equation (Businger, 1966; Dyer, 1967). With the development of observation technology, the coefficients in the BD equation have been further modified (e.g., Paulson, 1970; Webb, 1970; Businger et al., 1971; Dyer, 1974; Högström, 1996). In addition to the BD equation, some other schemes have been put forward and they may perform better especially for the strongly stable stratification (e.g., Holtslag and De Bruin, 1988, Beljaars and Holtslag, 1991, Chenge and Brutsaert, 2005). The schemes can be divided into two types according to the computing characteristics. One type is called as iterative algorithm (e.g., Paulson, 1970; Businger et al., 1971; Dyer, 1974; Högström, 1996; Beljaars and Holtslag, 1991), and it keep the MOST completely with less approximation so that the results can be more precise. However, it needs to take much more steps to converge and hence the CPU time is consuming which affects the ability and efficiency of modeling (Louis, 1979; Li et al., 2014); The other one is called as non-iterative algorithm (e.g., Louis et al., 1982; Launiainen, 1995; Wang et al., 2002; Wouters et al., 2012). Due to the approximate treatment, there is no need for loop iteration in calculation. It is much simpler and less CPU time-consuming, but it may lead to a lower accuracy of the results.

Although many researches above focused on the effects of the SL schemes on PBL and meteorological elements, few studies discussed it based on a pollution episode corresponding various atmospheric states. The turbulent exchange of momentum, heat, and moisture at the ground surface is more important than large-scale transport for the accumulation and transport of pollutants when atmosphere is stable. In this paper, two kinds of surface flux calculation schemes were compared and evaluated during a haze episode using observational flux data. One is a new scheme proposed by Li et al. (2014; 2015, Li hereinafter), the other is MM5 similarity scheme (Zhang and Anthes, 1982, MM5 hereinafter) which is widely applied in modeling investigation (e.g., Hu et al., 2010; Wang et al., 2015a, b; Tymvios et al., 2017). As a new one, the Li scheme is not yet applied to the atmosphere chemical models, and few relevant articles evaluate this scheme using the observational data especially in a haze episode. In this scheme, the aerodynamic roughness length z_{0m} and thermal roughness length z_{0h} are distinguished each other and the effect of the roughness sublayer (RSL) is taken into account. In addition, this scheme can be applied to the full range of roughness status $10 \leq \frac{z}{z_{0m}} \leq 10^5$ and $-0.5 \leq \ln\frac{z_{0m}}{z_{0h}} \leq 30$ under whole conditions $-5 \leq Ri_{\mathrm{B}} \leq 2.5$. Here z is the reference height and Ri_{B} is the bulk Richardson number. Compared with Li, the MM5 scheme does not consider the effect of both z_{0h} and the RSL. Further, in order to keep the stability of modeling, some limits have been used in MM5 such as a limit of -10 is used for both the stability parameter ζ and universal functions.

2 Theory

The definition of the momentum and sensible heat flux are introduced, and the detailed algorithms of the Li and MM5 schemes are explained.

2.1 Introduction of the momentum and sensible heat flux

The turbulent fluxes from ground surface are defined as follows:

$$\tau = \rho u_*^2 \quad \text{and} \tag{1a}$$

$$H = -\rho c_p u_* \theta_*. \tag{1b}$$

Where τ is the momentum flux, H is the sensible heat flux, ρ is the air density, c_p is the specific heat capacity at constant pressure. u_* and θ_* are the friction velocity and the temperature scale, respectively, and they represent the intensity of the vertical turbulent flux transport and they are approximately independent on height in the SL.

Both the Li and MM5 schemes are calculated with bulk flux parameterization. As an important dimensionless parameter related with the stability, the bulk Richardson number Ri_{B} is defined as

$$Ri_{\mathrm{B}} = \frac{gz(\theta-\theta_{\mathrm{g}})}{\theta u^2}. \tag{2}$$

Where g is the acceleration of gravity, z is the reference height which is the lowest level in the model, θ is the mean potential temperature at height z, θ_{g} is the surface radiometric potential temperature, u is the mean wind speed at height z. Thus, Ri_{B} can be computed through meteorological data at least two levels.

2.2 The Li scheme

The basic idea of Li is to parameterize ζ directly with Ri_{B}, z_{0m} and z_{0h}, and then calculate turbulence fluxes. In the scheme, bulk transfer coefficients of the momentum and sensible heat fluxes (C_M, C_H) are expressed as

$$C_M = \frac{u_*^2}{u^2} = \frac{\tau}{\rho u^2} \quad \text{and} \tag{3a}$$

$$C_H = \frac{u_*\theta_*}{u(\theta-\theta_{\mathrm{g}})} = -\frac{H}{\rho c_p u(\theta-\theta_{\mathrm{g}})}. \tag{3b}$$

Based on MOST and considering the RSL effect, the relationship between the bulk transfer coefficients and the profile functions corresponding to wind and potential temperature are usually expressed as

$$C_M = \frac{k^2}{\left[\ln\frac{z}{z_{0m}} - \psi_M\left(\frac{z}{L}\right) + \psi_M\left(\frac{z_{0m}}{L}\right) + \psi_M^*\left(\frac{z}{L}, \frac{z}{z_*}\right)\right]^2} \quad \text{and} \tag{4a}$$

$$C_H = \frac{k^2}{R\left[\ln\frac{z}{z_{0m}} - \psi_M\left(\frac{z}{L}\right) + \psi_M\left(\frac{z_{0m}}{L}\right) + \psi_M^*\left(\frac{z}{L}, \frac{z}{z_*}\right)\right]\left[\ln\frac{z}{z_{0h}} - \psi_H\left(\frac{z}{L}\right) + \psi_H\left(\frac{z_{0h}}{L}\right) + \psi_H^*\left(\frac{z}{L}, \frac{z}{z_*}\right)\right]}. \tag{4b}$$

Where k is the von Kármán constant which is 0.4 in both two schemes, R is the Prandtl number which is 1.0 in two schemes, ψ_M and ψ_H are the integrated stability functions for momentum and sensible heat, respectively, which are also called universe functions. L is the Obukhov length ($\zeta = \frac{z}{L}$), ψ_M^* and ψ_H^* are the correction functions accounting for RSL effect, z_* is the height of RSL. From above equations we can see that the calculation of the momentum and sensible heat flux requires C_M and C_H (or u_* and θ_*), and there are 3 key points to get them:

1. z_{0m} and z_{0h}. z_{0m} and z_{0h} are two key parameters in the bulk transfer equations and their definitions and influence will be given in Sect. 4.1.
2. ζ. In the Li scheme, the determination of ζ is the most crucial problem for calculation of turbulent fluxes. Li is a new scheme based on the results of Yang et al. (2001), Wouters et al. (2012), Sharan and Srivastava (2014), and which is proposed to approach the classic iterative computation results using multiple regressions. In particular, under stable conditions, the calculation procedure for a given group of Ri_{B}, z_{0m} and z_{0h} is the following: (1) find the region according to z_{0m} and z_{0h} with Table 1 (see Li et al., 2014); (2) find the section according to the region and Ri_{B} with Eq. (5) and coefficients in Table 2 (see Li et al., 2014); (3) calculate ζ using Eq. (6) and Tables 3-10 (see Li et al., 2014).

$$Ri_{\mathrm{Bcp}} = \sum C_{mn}(\log L_{0M})^m (L_{0H} - L_{0M})^n, \tag{5}$$

$$\zeta = Ri_{\mathrm{B}} \sum C_{ijk} Ri_{\mathrm{B}}^i L_{0M}^j (L_{0H} - L_{0M})^k. \tag{6}$$

Where C_{mn} and C_{ijk} are the coefficients in Tables 3-10. $L_{0M} = \ln\frac{z}{z_{0m}}$, $L_{0H} = \ln\frac{z}{z_{0h}}$. $m, n = 0, 1, 2$, and $m + n \leq 3$; $\mathrm{i, j, k} = 0, 1, 2, 3$, and $\mathrm{i + j + k} \leq 4$. Similarly, under unstable conditions, eight regions are divided according to the method from Li et al. (2015). For each of the regions, ζ is carried out by following:

$$\zeta = Ri_{\mathrm{B}} \frac{L_{0M}^{2}}{L_{0H}} \sum C_{ijk} \left(\frac{-Ri_{\mathrm{B}}}{1-Ri_{\mathrm{B}}}\right)^{i} L_{0M}^{-j}\, \mathrm{L}_{0H}{}^{-k}. \quad (7)$$

Where C_{ijk} is seen in Table 2 (Li et al., 2016), and $i = 0, 1$; $\mathrm{j}, \mathrm{k} = 0, 1, 2, 3$; $\mathrm{i} + \mathrm{j} + \mathrm{k} \le 4$.

3. Universal function. It is also a key factor in flux calculation. The form of universal function is adopted from CB05 (Chenge and Brutsaert, 2005) under the stable condition (Eqs. (8a), (8b)) and Paulson70 (Paulson, 1970) under the unstable condition (Eqs. (9a), (9b)):

$$\psi_M(\zeta) = -\mathrm{a} \ln\left[\zeta + (1 + \zeta^{b})^{\frac{1}{b}}\right], \quad \zeta > 0 \ \text{(stable)}, \quad (8a)$$

$$\psi_H(\zeta) = -\mathrm{c} \ln\left[\zeta + (1 + \zeta^{d})^{\frac{1}{d}}\right], \quad \zeta > 0 \ \text{(stable)}, \quad (8b)$$

$$\psi_M(\zeta) = 2 \ln\frac{1+x}{2} + \ln\frac{1+x^2}{2} - 2\arctan(x) + \frac{\pi}{2}, \quad \zeta < 0 \ \text{(unstable)}, \quad (9a)$$

$$\psi_H(\zeta) = 2\ln\frac{1+y}{2}, \quad \zeta < 0 \ \text{(unstable)}. \quad (9b)$$

Where $\mathrm{a} = 6.1$, $b = 2.5$, $\mathrm{c} = 5.3$, $d = 1.1$, $x = (1 - 16\zeta)^{1/4}$, $y = (1 - 16\zeta)^{1/2}$.

In addition, the RSL effect is taken into account in the Li scheme. In the RSL, turbulence is strongly affected by individual roughness elements, and the standard MOST is no longer valid (Simpson et al., 1998). Therefore, it is necessary to consider the RSL effect in the calculation of turbulent fluxes, especially for the rough terrain such as forest or large cities. Ridder (2010) proposed the expression of ψ_M^* and ψ_H^*:

$$\psi_M^*\left(\zeta, \ \frac{z}{z_*}\right) = \phi_M\left[\left(1 + \frac{\upsilon}{\mu_M z/z_*}\right)\zeta\right]\frac{1}{\lambda}\ln\left(1 + \frac{\lambda}{\mu_M z/z_*}\right)e^{-\mu_M z/z_*} \ \text{and} \quad (10a)$$

$$\psi_H^*\left(\zeta, \ \frac{z}{z_*}\right) = \phi_H\left[\left(1 + \frac{\upsilon}{\mu_H z/z_*}\right)\zeta\right]\frac{1}{\lambda}\ln\left(1 + \frac{\lambda}{\mu_H z/z_*}\right)e^{-\mu_H z/z_*}. \quad (10b)$$

Where $\upsilon = 0.5$, $\mu_M = 2.59$, $\mu_H = 0.95$, $z_* = 16.7 z_{0m}$, $\lambda = 1.5$. ϕ_M and ϕ_H are universal functions before integration. Here, set $\chi_M = 1 + \frac{\upsilon}{\mu_M z/z_*}$, $\chi_H = 1 + \frac{\upsilon}{\mu_H z/z_*}$:

$$\phi_M(\chi_M\zeta) = 1 + \mathrm{a}\frac{\chi_M\zeta + (\chi_M\zeta)^{b}\left[1 + (\chi_M\zeta)^{b}\right]^{\frac{1-b}{b}}}{\chi_M\zeta + \left[1 + (\chi_M\zeta)^{b}\right]^{\frac{1}{b}}}, \quad \zeta > 0 \ \text{(stable)}, \quad (11a)$$

$$\phi_H(\chi_H\zeta) = 1 + \mathrm{c}\frac{\chi_H\zeta + (\chi_H\zeta)^{d}\left[1 + (\chi_H\zeta)^{d}\right]^{\frac{1-d}{d}}}{\chi_H\zeta + \left[1 + (\chi_H\zeta)^{d}\right]^{\frac{1}{d}}}, \quad \zeta > 0 \ \text{(stable)}, \quad (11b)$$

$$\phi_M(\chi_M\zeta) = (1 - 16\chi_M\zeta)^{-1/4}, \quad \zeta < 0 \ \text{(unstable)}, \quad (12a)$$

$$\phi_H(\chi_H\zeta) = (1 - 16\chi_H\zeta)^{-1/2}, \quad \zeta < 0 \ \text{(unstable)}. \quad (12b)$$

The Li scheme is summarized as: firstly determine Ri_{B}、z_{0m} and z_{0h} according to the observation data, and then calculate ζ with Ri_{B}、z_{0m} and z_{0h}. Finally carry out the momentum and sensible heat fluxes under different stratification conditions.

2.3 The MM5 scheme

In this scheme, no distinction is made between z_{0m} and z_{0h}, thus we express the roughness length with z_0. Under the unstable condition, take Paulson70 with Eqs. (16a) and (16b), and under the stable condition, the atmospheric stratification conditions are subdivided into three cases according to Zhang and Anthes (1982). In addition, this scheme does not consider the RSL effect.

(1) Strongly stable condition ($Ri_{\mathrm{B}} \geq 0.2$):

$$\psi_M = \psi_H = -10 \ln \frac{z}{z_0}. \tag{13}$$

(2) Weakly stable condition ($0 < Ri_{\mathrm{B}} < 0.2$):

$$\psi_M = \psi_H = -5 \left(\frac{Ri_{\mathrm{B}}}{1.1 - 5Ri_{\mathrm{B}}} \right) \ln \frac{z}{z_0}. \tag{14}$$

(3) Neutral condition ($Ri_{\mathrm{B}} = 0$):

$$\psi_M = \psi_H = 0. \tag{15}$$

(4) Unstable condition ($Ri_{\mathrm{B}} < 0$):

$$\psi_M = 2 \ln \frac{1+x}{2} + \ln \frac{1+x^2}{2} - 2\arctan(x) + \frac{\pi}{2}, \tag{16a}$$

$$\psi_H = 2\ln \frac{1+y}{2}, \tag{16b}$$

where $x = (1 - 16\zeta)^{1/4}$, $y = (1 - 16\zeta)^{1/2}$.

This scheme calculates turbulent fluxes of the momentum and sensible heat with u_* and θ_*. In order to avoid the difference of u_* before and after is too large, u_* is arithmetically averaged with its previous value with Eq. (17), and a lower limit of $u_* = 0.1\mathrm{m/s}$ is imposed in order to prevent the heat flux from being zero under very stable conditions. According to the profile functions of wind and temperature near the ground, θ_* then is deduced by Eq. (18).

$$u_* = \frac{1}{2} \left(u_* + \frac{ku}{\ln \frac{z}{z_{0m}} - \psi_M} \right), \tag{17}$$

$$\theta_* = \frac{k(\theta - \theta_{\mathrm{g}})}{R[\ln \frac{z}{z_{0h}} - \psi_H]}. \tag{18}$$

Overall, the universal functions in different conditions are determined by Ri_{B} and z_0. Then u_* and θ_* will be calculated with meteorological data and flux data. At last, the turbulent fluxes are derived by Eqs. (1a) and (1b).

3 Observational data and methods

The observational data was from Gucheng station (GC), which is in China Atmosphere Watch Network (CAWNET) and located in the southwest of Beijing about 110km, at 115.40 °E, 39.08 °N. In winter, the station surface was covered with wheat and the surrounding areas were mainly farmland and scattered villages (Fig. 1). The eddy correlation flux measurement system is mainly composed of a three-dimensional (3D) Temperature measurement with a sonic anemometer

(CSAT3) and a fast response infrared gas analyzer (LI-7500) at 4m height. The data was collected from December 1, 2016 to January 9, 2017 including momentum fluxes, heat fluxes, wind speed and wind direction, air temperature, density of air and vapor, pressure with 30 minutes interval. Besides, there were radiation data provided by the net radiation sensor (CNR1) including the surface upward long wave radiation and the long wave radiation incident to the ground surface and $PM_{2.5}$ data provided by the Environmental Protection Station of China's Ministry of Environmental Protection (EPS/CMEP).

3.1 Data processing

In order to obtain accurate flux data, it needs quality control of the observational data, including eliminated the outliers and the data in rainy days, as well as correcting momentum by using a double axis rotation for the sonic anemometer tilt correction and correcting sensible heat fluxes by modifying sonic virtual temperature. In addition, we considered the effect of wind field on the roughness length. Fig. 2 shows distribution frequency of wind speed and wind direction at GC during observations (December 1, 2016 ~ January 9, 2017). The wind speed is stable during this period and the maximum is no more than 5m and most of them are about 1 ~ 2m/ s. The wind direction is relatively uniform except for the southeast wind (135 degrees). Therefore, to avoid the measurement error of the instrument, the wind speed data less than 0.5m/s are eliminated.

3.2 Determination of surface skin temperature

The surface skin temperature error caused by the CSAT3 is too large to be taken to calculate the flux as input. Therefore, the surface skin temperature is calculated from the radiation data detected by the CNR1 as:

$$R_{lw}^{\uparrow} = (1-\varepsilon_s)R_{lw}^{\downarrow} + \varepsilon_s \sigma T_g^4, \tag{19}$$

where $R_{lw}^{\uparrow}$ and $R_{lw}^{\downarrow}$ are the surface upward longwave radiation and long wave radiation incident on the surface, respectively. σ is the Stephen Boltzmann constant, $\sigma = 5.67\times10^{-8}\mathrm{Wm^{-2}K^{-4}}$. T_g is the surface skin temperature, ε_s is the surface emissivity which is the basis for calculating T_g. Many researches estimated ε_s and the range of the values is always 0.9 ~ 1 (Stewart et al., 1994; Verhoef et al., 1997). According to the semi-empirical method in Yang et al. (2008), ε_s is estimated when the RMSE is minimal. In this paper, the Li and MM5 schemes were used to estimate the ε_s value (as shown in Fig. 3). It is clear that the ε_s value corresponding the minimum RMSE is not very sensitive to the choice of two schemes. When ε_s is 1, the RMSE has the minimum value. Thus, we take 1 as the optimal value of ε_s to calculate T_g value.

4 Results and discussion

The concept of roughness and its influence on the calculation of turbulent flux are going to be described in detail, and then the value of z_{0m} and z_{0h} will be determined by theories above. Using z_{0m}, z_{0h} and related observational data, we

Atmos. Chem. Phys. Discuss., https://doi.org/10.5194/acp-2018-247
Manuscript under review for journal Atmos. Chem. Phys.
Discussion started: 25 April 2018

will have offline tests on Li and MM5. Finally, the behavior of two schemes will be compared in a severe haze pollution at GC.

4.1 The influence of roughness length on the calculation of turbulent flux

z_{0m} is defined as a height at which the extrapolated wind speed following the similarity theory vanishes. It is mainly determined by land-cover type and canopy height after excluding large obstructions. In models, z_{0m} is always based on a look-up table which is related to land-cover type. In this paper, z_{0m} is simply classified based on the research of Stull (1988) and is listed in Table 1. It can be seen that the more rough land surface is, the higher value of z_{0m} is. Thus, different land-cover types have different effects on flux calculation. z_{0h} is a height at which the extrapolated air temperature is identical to the surface skin temperature, and it is also a scalar quantity. Some early researches assumed that z_{0m} was equal to z_{0h} (Louis, 1979; Louis et al., 1982). However, the assumption is not applicable in reality because z_{0m} and z_{0h} have different physical meanings. Thus, many following studies modified this assumption and made it more reliable in the situation that z_{0m} was not equal to z_{0h} or the difference between two values was much large (e.g., Song, 1998; Wouters et al., 2012; Li et al., 2014; Li et al., 2015).

With the Li scheme, we test the effect of the roughness length on flux calculation. In the process, take $z = 10\text{m}$ as the reference height and set the range of Ri_{B} according to Louis82 (Louis et al., 1982) from -2 to 1. Firstly, discuss the effect of z_{0m} on flux calculation. Set $\frac{z_{0m}}{z_{0h}} = 1$, corresponding to four cases: z_{0m}= 1, 0.5, 0.05, 0.001m. These cases correspond to large cities, forests, agricultural fields and wide water surface, respectively. Fig. 4 gives the relationship between $C_M(C_H)$ and Ri_{B} for different z_{0m} values. The effects of different land-cover types on C_M and C_H are significant under both the stable atmosphere ($Ri_{\mathrm{B}} > 0$) and the unstable atmosphere ($Ri_{\mathrm{B}} < 0$). The rougher the surface is (corresponding the larger z_{0m} value), the larger the calculated momentum or sensible heat flux is. In addition, there is a corresponding relationship between $C_M(C_H)$ and stability. The more unstable the atmosphere is, the larger difference the value of $C_M(C_H)$ is and vice versa. Once the value of Ri_{B} exceeds the critical value (generally 0.2~0.25), the transfer coefficients decline sharply but above 0.

Secondly, discuss the effect of difference between z_{0m} and z_{0h} on flux calculation. The relationship between z_{0m} and z_{0h} can be expressed as $kB^{-1} = \ln\frac{z_{0m}}{z_{0h}}$. Over the sea, z_{0m} is comparable to z_{0h}; over the uniform vegetation surface (e.g., grassland, farmland, woodland), kB^{-1} is about 2 ($z_{0m}/z_{0h} \approx 10$) (Garratt and Hicks, 1973; Garratt, 1978; Garratt and Francey, 1978); over the surface with bluff roughness elements, the $\frac{z_{0m}}{z_{0h}}$ value may be very large. For example, in some large cities, kB^{-1} can reach 30 ($z_{0m}/z_{0h} \approx 10^{13}$) (Sugawara and Narita, 2009). Therefore, the $\frac{z_{0m}}{z_{0h}}$ value can varies over a wide range. Fig. 5 shows the relationship between $C_M(C_H)$ and Ri_{B} for different $\frac{z_{0m}}{z_{0h}}$ values. Set $z_{0m} = 1$, z_{0h}=1, 0.01,

10^{-4}, 10^{-6}m, and The large difference derived from the different ratios in Fig. 5. The larger the ratio is, the slower $C_M(C_H)$ fails with a rising stability. These results show that distinguishing between z_{0m} and z_{0h} has great impact on flux calculation which is closely related to severe haze pollution. Ignoring the difference between the two may lead to large errors in flux calculation and finally in air quality modeling.

4.2 The determination of roughness length z_{0m} (z_{0h})

Based on above description and discussion, it can be seen that the determination of the appropriate value of z_{0m} (z_{0h}) is a key and basis for calculation of surface turbulent fluxes. Using observational flux data with quality control, z_{0m} and z_{0h} are derived by Eq. (20a) and (20b) following Yang et al. (2003) and Sicart et al. (2014).

$$\frac{u_*}{u} = \frac{k}{\ln\frac{z}{z_{0m}} - \psi_M}, \tag{20a}$$

$$\frac{\theta_*}{(\theta - \theta_g)} = \frac{k}{R[\ln\frac{z}{z_{0h}} - \psi_H]}. \tag{20b}$$

During the observation period, the crops stopped growing and the height did not exceed 0.1 m, so the zero-plane displacement height can be ignored. The observation time is too short (about 1 month) to consider the effect of seasonal variations on roughness. Thus, assume z_{0m} and z_{0h} are two fixed values. Given the observational data, a dataset of z_{0m} (z_{0h}) then is generated. Finally take median of the dataset as typical values of z_{0m} and z_{0h} for GC site: $z_{0m} = 0.0419$m, $z_{0h} = 0.0042$m. These results are comparable to the typical values for agricultural fields ($z_{0m} = 0.05$, $z_{0m}/z_{0h} = 10$) discussed above. Therefore, the results are considered credible.

4.3 Comparison of two schemes for calculating momentum and sensible heat flux

Using the calculated roughness length and the relative observations, the Li and MM5 schemes are going to be tested offline to compare their calculations of the momentum and sensible heat flux (Fig. 6). Firstly, take $z_{0m} = 0.0419$ and $z_{0h} = 0.0042$ in the Li scheme, $z_0 = z_{0m} = 0.0419$ in the MM5 scheme to calculate the momentum and sensible heat fluxes and the comparison results are shown in Figs. 6a and 6b. Compared with MM5, Li performs better with higher regression coefficient and determination coefficient. For momentum fluxes, the regression coefficient in Li is 0.6795 and that in MM5 is 0.5598, indicating that the error of Li is 12% lower than that of MM5. For sensible heat fluxes, the regression coefficient in Li is 0.7967 and that in MM5 is 1.7994. The latter is much larger than 1 which says the MM5 scheme overestimate a lot. That is due to no distinction of roughness length in the MM5 scheme. In order to compare the difference of two schemes without considering the effect of roughness length, take $z_0 = z_{0h} = 0.0042$ in the MM5 scheme to calculate the sensible heat fluxes as Fig. 6c. Compared with Fig. 6b, there is a great improvement after modifying z_0 value that the regression coefficient in MM5 becomes 0.7363, which is indicated that the error of calculated sensible heat flux by MM5 was reduced by 54% after discriminating z_{0h} from z_{0m}. However, the error in Li is still 5% lower than that in MM5.

This illustrates that in addition to the effect of roughness length, the Li scheme itself (including the selection of universal functions and the consideration of the RSL effect) is more reasonable than the MM5 scheme.

4.4 The specific performance of the two scheme in severe haze pollution

There were two obvious pollution processes during this observation period and one occurred during December 13 to 23, 2016. Fig. 7 shows the time series of $PM_{2.5}$ as well as the momentum fluxes and sensible heat fluxes both for calculation and observation in this pollution episode. For the research purpose significance, only the variation of above variables in the daytime (set from 8:00 a.m. to 20:00 p.m.) is taken into account. All analysis data are processed as hourly average. It needs to note that in MM5, take 0.0419 of z_0 when calculate momentum fluxes and take 0.0042 of z_0 when calculate sensible heat fluxes. As shown in Fig. 7, on the whole, the calculated results of momentum and sensible heat fluxes for the two schemes are consistent with the trend of the observed data. Specifically, for the momentum fluxes (Fig. 7a), when the observed momentum fluxes are large, the calculated results of the two schemes have little difference. When the observed momentum fluxes are small, the Li scheme results are close to or less than the observations, while the MM5 scheme results are always higher than observations because of the limit of $u_* = 0.1$. For the sensible heat fluxes (Fig. 7b), MM5 results are always lower than observations while Li results are closer to observations especially when the observed values are small.

Fig. 7 also shows the diurnal variation of $PM_{2.5}$ during this process. According to the evolution characteristics of fluxes and $PM_{2.5}$ concentration, the process is then divided into three stages: the no pollution stage (stage 1: 13~14), the accumulation stage (stage 2: 16~18) and the maintenance stage (stage 3: 21~22) to discuss and evaluate the two schemes. As shown in Fig. 7, before the pollution occurs (stage 1), the atmospheric stratification is unstable, $PM_{2.5}$ concentration is low and there is a strong flux transport in the SL, the corresponding observations of the momentum and sensible heat flux are relatively high and the daily change of them is also great. In the accumulation stage (stage 2), the atmosphere is changing from unstable to stable corresponding with hazes formation, the momentum and sensible heat fluxes gradually decreases and the daily variation also decreases. In the maintenance stage, the atmospheric stratification is very stable, and flux transport in the SL is weak, both the momentum and sensible heat fluxes are at a low level.

Fig. 8 shows the probability distribution functions (PDF) of the difference of momentum (Figs. 8a, 8c, 8e, 8g) and sensible heat fluxes (Figs. 8b, 8d, 8f, 8h) calculated by using Li and MM5 schemes from the observations in different stages. In the whole pollution process, for momentum fluxes (Fig. 8a), compared with MM5, the distribution of bias from the Li scheme tends to cluster in a narrower range centered by 0, and the probability of Li bias within ±0.005N m^{-2} is 46.82%. The probability of MM5 bias within this range fall to 23.02%. For sensible heat fluxes (Fig. 8b), the distribution of bias from Li is still more concentrated around 0 than it is from MM5. The probabilities of Li and MM5 bias within ±2.5W m^{-2} are 32.54% and 13.49%, respectively. In stage 1, for momentum fluxes (Fig. 8c), the probability of Li bias within ±0.005N m^{-2} is 38.09%. The probability distribution of MM5 bias focus on area larger than 0, and its probability within ±0.005N m^{-2} is 14.29%. For sensible heat fluxes (Fig. 8d), the probability of Li bias within ±2.5W m^{-2} is 38.09%, the same as momentum fluxes. The probability distribution of MM5 bias focus on area less than 0, and its probability within ±2.5W m^{-2} is 9.52%. In stage 2, the difference between the schemes is more obvious. The momentum and sensible heat fluxes bias from Li is the most concentrated around 0 in all cases, while the distribution of MM5 bias is similar to that in stage 1. Specifically, for momentum fluxes (Fig. 8e), the probabilities of Li bias and MM5 bias within ±0.005N m^{-2} are 56.25% and 25.00%. For sensible heat fluxes (Fig. 8f), the probabilities of Li bias and MM5 bias within ±2.5W m^{-2} are 40.62% and 6.25%. In stage 3, the difference between two schemes is small. For momentum fluxes (Fig. 8g), the probabilities of Li bias and MM5 bias within ±0.005N m^{-2} are 22.73% and 27.27%. For sensible heat fluxes (Fig. 8h), the probabilities of Li bias and MM5 bias within ±2.5W m^{-2} are both 36.36%.

Four common evaluation metrics were used to further test the abilities of the Li and MM5 schemes in calculating fluxes (Table 2). They are the mean bias (MB), normalized mean bias (NMB), normalized mean error (NME) and root mean square error (RMES). Table 2 shows that the Li scheme generally gives a better estimate than the MM5 scheme. In whole process, the momentum fluxes calculated by Li is underestimated by 3.63% relative to the observations, while the results calculated by MM5 is overestimated by 34.03%. The sensible heat fluxes calculated by Li and MM5 are both underestimated and the underestimations are 15.69% and 50.22%. In three selected stages, the Li scheme performs better than the MM5 scheme in first two stages. Especially in stage 2, that is, the atmosphere transforming from unstable to stable stratification, the difference between the Li and MM5 schemes are particularly significant. Both the Li and MM5 schemes have overestimates for momentum fluxes and the values are 7.68% and 45.56, respectively. Two schemes have underestimates for sensible heat fluxes and the values are 33.84% and 76.88%. It can be seen the Li scheme calculation error is much smaller than the MM5 scheme error. This stage plays an important role in the generation and accumulation of pollutants. How to simulate the atmospheric state in a more reasonable way is also a critical issue for air pollution modeling. Therefore, the superiority of the Li scheme in the air pollution process, especially in this stage is of great reference value for improving the forecast of pollutant concentration in the current air quality model. In stage 3, the difference between the two schemes is not obvious.

5 Conclusions

The applicability in describing the atmospheric stratification related with severe haze in east China of the Li and MM5 schemes are evaluated and discussed. The observed momentum and sensible heat fluxes, together with conventional meteorological data from December 1, 2016 to January 9, 2017, including a severe pollution episode from December 13 to 23, are used to do that. The transitional stage of atmospheric stratification from unstable to stable, corresponding to accumulation of $PM_{2.5}$, is mainly discussed in this paper. The contributions of roughness lengths (z_{0m} and z_{0h}) as well as the algorithms of the momentum and sensible heat flux calculation are discussed. The results are summarized as follows:

1) z_{0m} and z_{0h} have important effects on turbulent flux calculation. z_{0m} and $\frac{z_{0m}}{z_{0h}}$ both reflect the condition of underlying surface and impact flux calculation greatly. Under the same condition, the larger z_{0m} (indicating rougher surface) is, the larger the calculated fluxes are. The fluxes over large cities ($z_{0m} = 1$) is quite different from those over agricultural fields ($z_{0m} = 0.05$, similar to the value at GC). When z_{0m} is larger, the value of $\frac{z_{0m}}{z_{0h}}$ should be larger, and the larger the value of $\frac{z_{0m}}{z_{0h}}$ is, the greater the differences of calculated fluxes are. Especially, for a super city like Beijing, the value of $\frac{z_{0m}}{z_{0h}}$ may be much larger than 10^6 and ignoring the difference between z0m and z0h may lead to much uncertainties in flux calculation. It is very necessary to distinguish between z_{0m} and z_{0h} in SL scheme, which is probably beneficial to improve simulation of regional atmosphere stratification over urban agglomeration with rough surface and then $PM_{2.5}$ during hazes.

2) It could be seen from the regression coefficients and determination coefficients between calculated fluxes by the two schemes and observed fluxes of 40 days that the Li scheme was better than the MM5 scheme in general. For the momentum fluxes, the determination coefficients of Li and MM5 was about 0.41 and 0.40. Both schemes passed the significance level of 99.9%. The regression coefficient of Li was 0.68, and it generally reduced the error by 12% compared with MM5. When z_{0m} and z_{0h} took the same value ($z_0 = z_{0m} = 0.0419$) in MM5, the sensible heat fluxes were obvious overestimated. When z_{0h} was taken into account ($z_0 = z_{0h} = 0.0042$) in MM5, the calculated fluxes were significant improved and the error was reduced by 54%. However, this error was still higher about 5% compared with the Li scheme, illustrating that apart from the impact of roughness length, the different algorithms of the two schemes also achieves obvious differences in calculated fluxes.

3) During the heavy pollution process, the calculated momentum and sensible heat fluxes by the Li scheme were better than those by the MM5 scheme generally. Especially in the PM2.5 accumulated stage, the advantages of Li were more prominent. Compared with MM5, the probability distributions of both the momentum and sensible heat flux bias of Li tended to cluster in a narrower range centered by 0. The calculated momentum fluxes by Li were overestimated by 7.68% and this overestimation by MM5 was up to 45.56%. The calculated sensible heat fluxes by Li were underestimated by 33.84% while this underestimation by MM5 was even up to 76.88%.

The offline study in this paper showed that Li scheme was superior to the MM5 scheme in general. This superiority was even more remarkable during the atmosphere transforming stage from unstable to stable stratification. However, the comparison of the two schemes focusing on more underlying surfaces (e.g., super cities and agricultural fields) could not be conducted at present due to the shortage of observed fluxes data, which should be discussed in detail in next paper when the sufficient data is available. The offline results of this paper only offer a basic and a possible way to improve PBL diffusion simulation and then $PM_{2.5}$ prediction, which will be achieved in the follow-up work of online integrating of the Li scheme into the atmosphere chemical model.

Acknowledgments

The study was supported by National Key Project of HePAP. (JFYS2016ZY01002213), the National (Key) Basic Research and Development (973) Program of China (2014CB441201), National Key R & D Program Pilot Projects of China (2016YFC0203304)

References

Ban, J.M., Gao, Z.Q., Lenschow, D. H., 2010. Climate simulations with a new air-sea turbulent flux parameterization in the National Center for Atmospheric Research Community Atmosphere Model (CAM3). J. Geophys. Res. 115.

Beljaars, A.C.M., Holtslag, A.A.M., 1991. Flux parameterization over land surfaces for atmospheric models. J. Appl. Meteor. 30, 327-341.

Businger, J.A., 1966. Transfer of momentum and heat in the planetary boundary layer. in Proceedings of a Symposium on Arctic Heat Budget and Atmospheric Circulation. 305-331. The RAND Corp., Santa, Monica, Calif.

Businger, J.A., Wyngaard, J.C., Izumi, Y., Bradley, E. F., 1971. Flux-profile relationships in the atmospheric surface layer. J.Atmos. Sci. 28, 181-189.

Chenge, Y., Brutsaert, W., 2005. Flux-profile relationships for wind speed and temperature in the stable atmospheric boundary layer. Bound.-Layer Meteorol. 114, 519-538.

Cheng, F.Y., Chin, S.C., Liu, T.H., 2012. The role of boundary layer schemes in meteorological and air quality simulations of the Taiwan area. Atmos. Environ. 54, 714-727.

Dyer, A.J., 1967. The turbulent transport of heat and water vapour in an unstable atmosphere. Quart. J. Roy. Meteor. Soc. 93, 501-508.

Dyer, A.J., 1974. A review of flux-profile relationships. Bound.-Layer Meteorol. 7, 363-372.

Garratt, J.R., 1978. Transfer characteristics for a heterogeneous surface of large aerodynamic roughness. Quart. J. Roy. Meteor. Soc. 104, 491-502.

Garratt, J.R., Hicks, B.B., 1973. Momentum, heat and water vapour transfer to and from natural and artificial surfaces. Quart. J. Roy. Meteor. Soc. 99, 680-687.

Garratt, J.R., Francey, R.J., 1978. Bulk characteristics of heat transfer in the unstable, baroclinic atmospheric boundary layer. Bound.-Layer Meteorol. 15, 399-421.

Högström, U., 1996. Review of some basic characteristics of the atmospheric surface layer. Bound.-Layer Meteorol. 78, 215-246.

Atmos. Chem. Phys. Discuss., https://doi.org/10.5194/acp-2018-247
Manuscript under review for journal Atmos. Chem. Phys.
Discussion started: 25 April 2018

Holtslag, A.A.M., de Bruin, H.A.R., 1988. Applied modeling of the nighttime surface energy balance over land. J. Appl. Meteor. 27, 689-704.

Hu, X.M., Nielsen-Gammon, J.W., Zhang, F.Q., 2010. Evaluation of three planetary boundary layer schemes in the WRF model. J. Appl. Meteorol. Climatol. 49, 1831-1844.

Jiménez, P.A., Dudhia, J., González-Rouco, J.F., Navarro, J., Montávez, J.P., García-Bustamante, E., 2012. A revised scheme for the WRF surface layer formulation. Mon. Wea. Rev. 140, 898-918.

Launiainen, J., 1995. Derivation of the relationship between the Obukhov stability parameter and the bulk Richardson number for flux-profile studie. Bound.-Layer Meteorol. 76, 165-179.

Li, Y.B., 2014. On the Surface Turbulent Fluxes Calculation in Numerical Models. Beijing: university of Chinese academy of sciences.

Li, Y., Gao, Z., Li, D., Wang, L., Wang, H., 2014. An improved non-iterative surface layer flux scheme for atmospheric stable stratification conditions. Geosci. Model Dev. 7, 515-529.

Li, Y., Gao, Z., Li, D., Chen, F., Yang, Y., Sun, L., 2015. An Update of Non-iterative Solutions for Surface Fluxes Under Unstable Conditions. Bound.-layer Meteorol. 156, 501-511.

Li, Y., Gao, Z., Li, D., Chen, F., Yang, Y., Sun, L., 2016. Erratum to: An Update of Non-iterative Solutions for Surface Fluxes Under Unstable Conditions. Bound.-Layer Meteorol. 161: 225-228.

Louis, J. F.,1979. A parametric model of vertical eddy fluxes in the atmosphere. Bound.-Layer Meteorol. 17, 187-202.

Louis, J. F., Tiedtke, M., Geleyn, J. F., 1982. A short history of the operational PBL parameterization at ECMWF [C]// Proc. Workshop on Planetary Boundary Layer Parameterization. Shinfield Park, Reading, Berkshire, UK, European Centre for Medium Range Weather Forecasts. 59-79.

Monin, A., Obukhov, A., 1954. Osnovnye zakonomernosti turbulentnogo peremesivanjia v prizemnon sloe atmosfery (Basic laws of turbulent mixing in the atmosphere near the ground). Trudy geofiz. inst. AN SSSR. 24, 163–187.

Paulson, C. A., 1970. The mathematical representation of wind speed and temperature profiles in the unstable atmospheric surface layer. J. Appl. Meteorol. 9, 857-861.

Ridder, K.D., 2010. "Bulk Transfer Relations for the Roughness Sublayer." Bound.-Layer Meteorol. 134, 257-267.

Sharan, M., Srivastava, P., 2014. A Semi-Analytical Approach for Parametrization of the Obukhov Stability Parameter in the Unstable Atmospheric Surface Layer. Bound.-Layer Meteorol. 153, 339-353.

Sicart, J.E., Litt, M., Helgason, W., Tahar, V.B., Chaperon, T., 2014. A study of the atmospheric surface layer and roughness lengths on the high-altitude tropical Zongo glacier, Bolivia. J. Geophys. Res. 119, 3793–3808.

Simpson, I.J., Thurtell, G.W., Neumann, H.H., Den Hartog, G., Edwards, G.C., 1998. The Validity of Similarity Theory in the Roughness Sublayer Above Forests. Bound.-Layer Meteorol. 87, 69-99.

Song, Y., 1998. An Improvement of the Louis Scheme for the Surface Layer in an Atmospheric Modelling System. Bound.-Layer Meteorol. 88, 239-254.

Stewart, J. B., Kustas, W. P., Humes, K. S., Nichols, W. D., Moran, M. S., de Bruin, H. A. R., 1994. Sensible Heat Flux-Radiometric Surface Temperature Relationship for Eight Semiarid Areas. J. Appl. Meteorol. 33, 1110-1117.

Stull, R. B., 1988. An Introduction to Boundary Layer Meteorology, Kluwer Academic Publishers. Dordrecht.

Sugawara, H., Narita, K., 2009. Roughness length for heat over an urban canopy. Theor. Appl. Climatol. 95, 291-299.

Tymvios, F., Charalambous, D., Michaelides, S., Lelieveld, J., 2017. Intercomparison of boundary layer parameterizations for summer conditions in the eastern Mediterranean island of Cyprus using the WRF-ARW model. Atmos. Res. DOI: 10.1016/j.atmosres.2017.09.011.

Verhoef, A., de Bruin, H. A. R., van den Hurk, B. J. J. M., 1997. Some Practical Notes on the Parameter kB1 for Sparse Vegetation. J. Appl. Meteorol. 36, 560-572.

Wang, S., Wang, Q., Doyle, J., 2002. Some improvement of Louis surface flux parameterization. Preprints, 15th Symp. on Boundary Layers and Turbulence, Wageningen, Netherlands, Amer. Meteor. Soc., 547–550.

Wang, H., Xue, M., Zhang, X. Y., Liu, H. L., Zhou, C. H., Tan, S. C., Che, H. Z., Chen, B., Li, T., 2015a. Mesoscale modeling study of the interactions between aerosols and PBL meteorology during a haze episode in Jing-Jin-Ji (China) and its nearby surrounding region - Part 1: Aerosol distributions and meteorological features. Atmos. Chem. Phys. 15,3257-3275.

Wang, H., Shi, G. Y., Zhang, X. Y., Gong, S. L., Tan, S. C., Chen, B., Che, H. Z., Li, T., 2015b. Mesoscale modeling study of the interactions between aerosols and PBL meteorology during a haze episode in China Jing-Jin-Ji and its near surrounding region - Part 2: Aerosols' radiative feedback effects. Atmos. Chem. Phys. 15, 3277-3287.

Webb, E. K., 1970. Profile relationships: The log-linear range, and extension to strong stability. Quart. J. Roy. Meteor. Soc. 96, 67-90.

Wouters, H., De Ridder, K., van Lipzig, N. P. M., 2012. Comprehensive Parametrization of Surface-Layer Transfer Coefficients for Use in Atmospheric Numerical Models. Bound.-Layer Meteorol. 145, 539-550.

Xie, B., Fung, J. C. H., Chan, A., Lau, A., 2012. Evaluation of nonlocal and local planetary boundary layer schemes in the WRF model. J. Geophys. Res. 117(D12), 48-50.

Yang, K., Tamai, N., Koike, T., 2001. Analytical Solution of Surface Layer Similarity Equations. J. Appl. Meteorol. 40, 1647-1653.

Yang, K., Koike, T., Yang, D., 2003. Surface Flux Parameterization in the Tibetan Plateau. Bound.-Layer Meteorol. 106, 245-262.

Yang, K., Koike, T., Ishikawa, H., Kim, J., Li, X., Liu, H. Z., Liu, S. M., Ma, X. M., Wang, J. M., 2008. Turbulent Flux

Transfer over Bare-Soil Surfaces: Characteristics and Parameterization. J. Appl. Meteorol. CLIM. 47, 276-290.

Zhang, D., Anthes, R. A., 1982. A high-resolution model of the planetary boundary layer—Sensitivity tests and comparisons with SESAME-79 data. J. Appl. Meteorol. 21, 1594-1609.

Atmos. Chem. Phys. Discuss., https://doi.org/10.5194/acp-2018-247
Manuscript under review for journal Atmos. Chem. Phys.
Discussion started: 25 April 2018

449 **Table 1.** Typical values of z_{0m} corresponding to various land-cover types

z_{0m}/m	Land-cover types
5~50	Mountain (above 100m)
1~5	The center of large cities, hills or mountain area
0.1~1	Forests, the center of large towns
0.01~0.1	Flat grasslands, agricultural fields
10^{-4}~10^{-3}	The snow surface, wide water surface, flat deserts
10^{-5}	The ice surface

450
451
452
453 **Table 2.** Statistics between the Li and MM5 schemes calculated turbulent flux.

		Li				MM5			
		MB	NMB	NME	RMSE	MB	NMB	NME	RMSE
Whole process	τ	-0.0006	-3.63%	54.29%	0.0142	0.0058	34.03%	63.59%	0.0143
	H	-2.2723	-15.69%	52.73%	10.9649	-7.2735	-50.22%	69.68%	12.7946
Stage 1	τ	0.0021	9.98%	55.90%	0.0172	0.0091	43.45%	66.66%	0.0169
	H	1.1775	5.79%	37.87%	10.5734	-7.1891	-35.34%	55.70%	13.1324
Stage 2	τ	0.0013	7.68%	44.50%	0.0111	0.0079	45.56%	56.81%	0.0121
	H	-4.5752	-33.84%	50.28%	9.3995	-10.3924	-76.88%	81.40%	13.2553
Stage 3	τ	-0.0024	-13.25%	59.13%	0.0144	0.0030	16.72%	56.34%	0.0138
	H	1.2818	11.39%	66.31%	11.4778	-1.7479	-15.52%	65.90%	10.4219

454 ∗ τ: momentum flux; H: sensible heat flux; MB: mean bias; NMB: normalized mean bias; NME: normalized mean error;
455 RMSE: root mean square error. The units of MB and RMSE: $\mu g \cdot m^{-3}$.
456

Atmospheric Chemistry and Physics
Discussions
Open Access

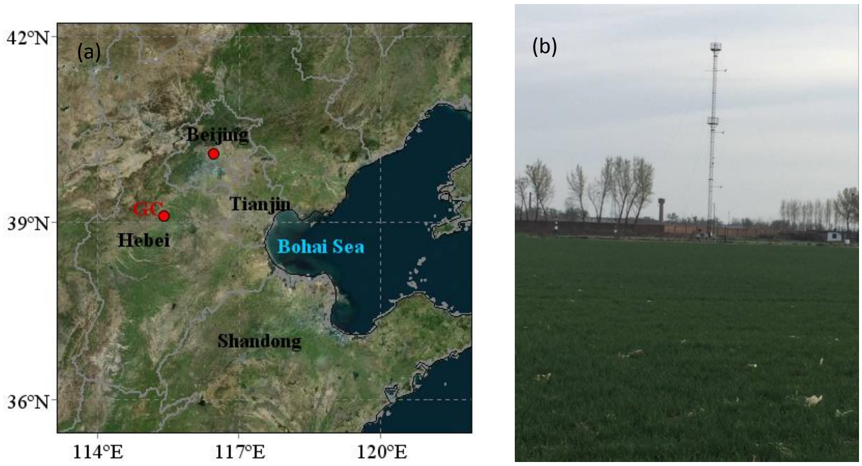

Figure 1. Location (a) and geographical environment (b) at GC. The map is from Bing Maps.

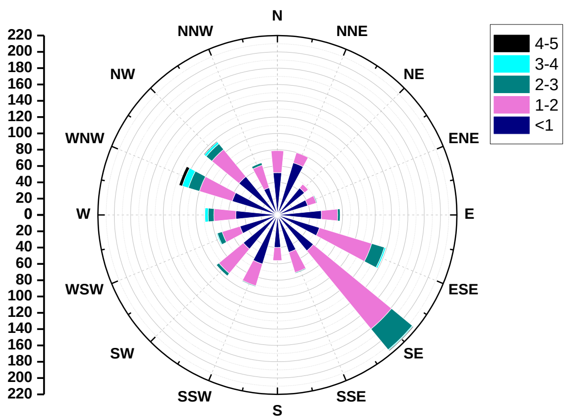

Figure 2. Wind Rose map at GC from December 1, 2016 to January 9, 2017.

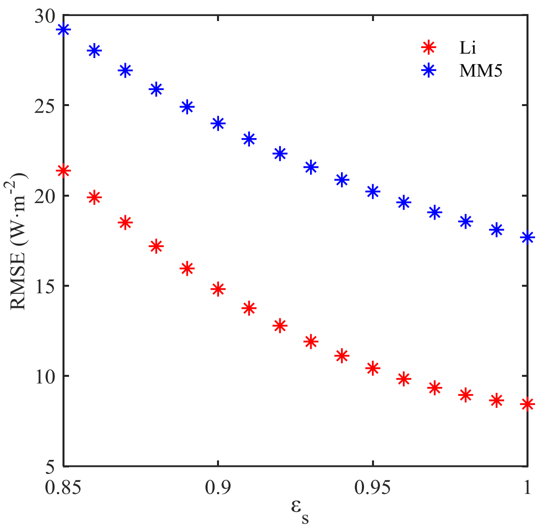

Figure 3. The surface emissivity ε_s dependence of RMSE between observed near-neutral heat fluxes and parameterized heat fluxes (red for Li and blue for MM5) at GC.

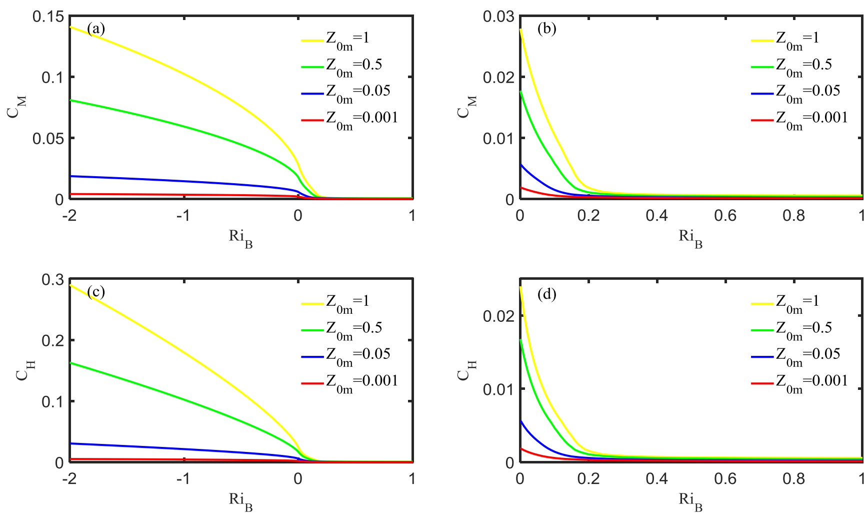

Figure 4. The relationship between $C_M(C_H)$ and Ri_B for different z_{0m} values.

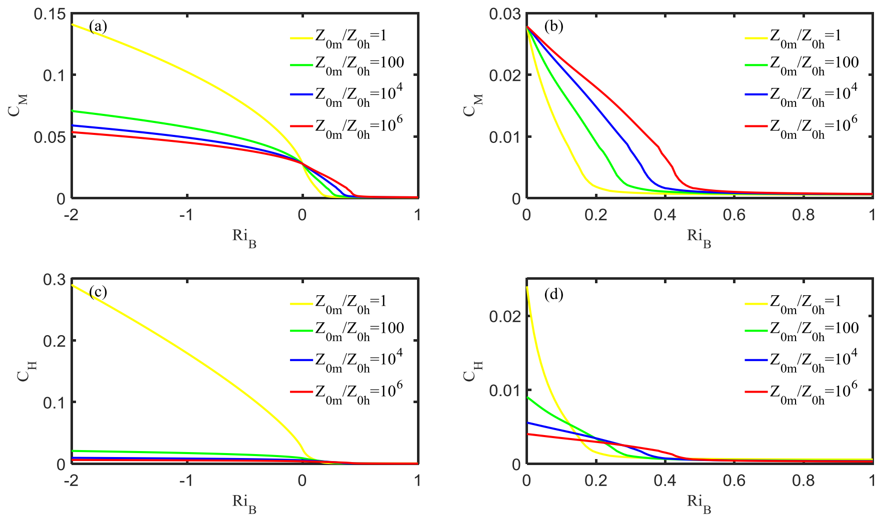

Figure 5. The relationship between $C_M(C_H)$ and Ri_B for different ratios of z_{0m} to z_{0h}.

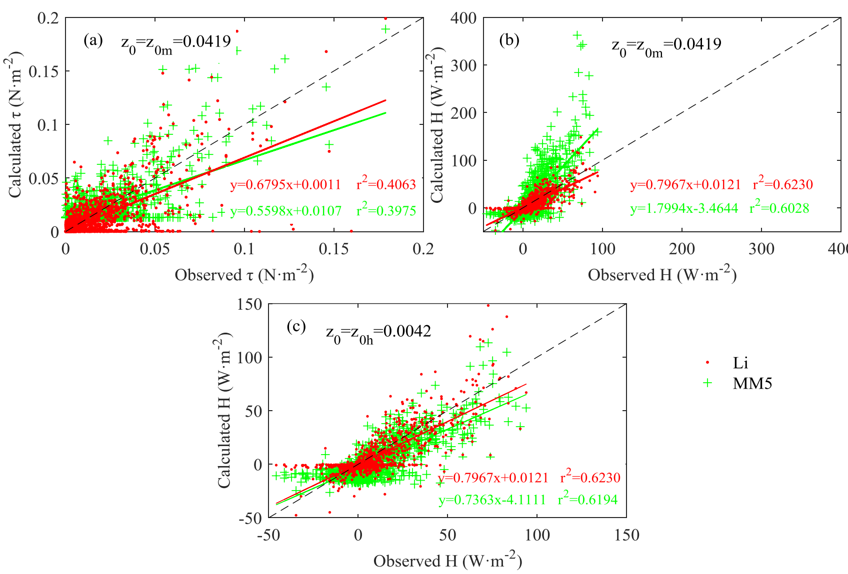

Figure 6. Comparison of calculated and observed fluxes. (a) Momentum fluxes (MM5: z_0 = 0.0419); (b) sensible heat fluxes (MM5: z_0 = 0.0419); (c) sensible heat fluxes (MM5: z_0 = 0.0042). Red dots: the Li scheme; green plus signs: the MM5 scheme.

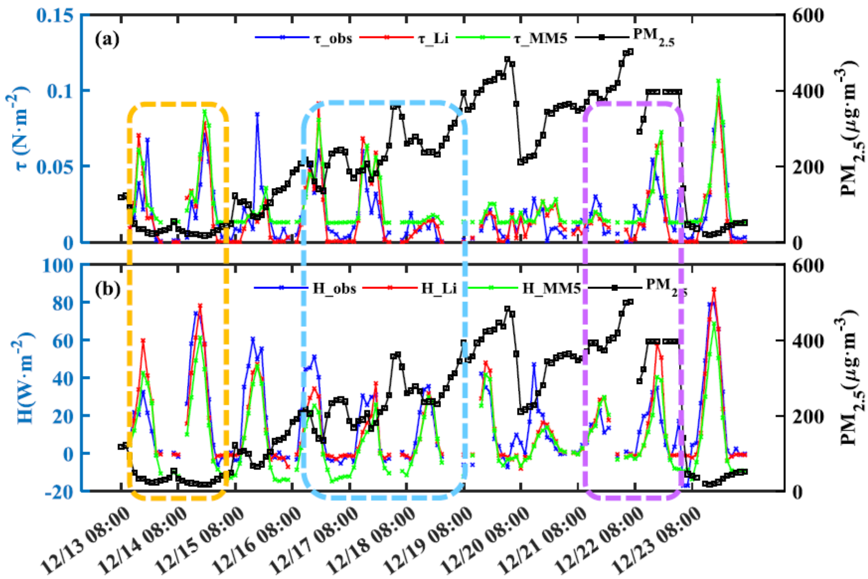

Figure 7. Variations of hourly turbulent fluxes and $PM_{2.5}$ at GC station in daytime. (a) Momentum fluxes τ (blue line: observations; red line: the Li scheme; green line: the MM5 scheme) and $PM_{2.5}$ concentration (black line); (b) sensible heat fluxes H (the same as τ) and $PM_{2.5}$ concentration (black line). Yellow box: stage 1; blue box: stage 2; purple box: stage 3.

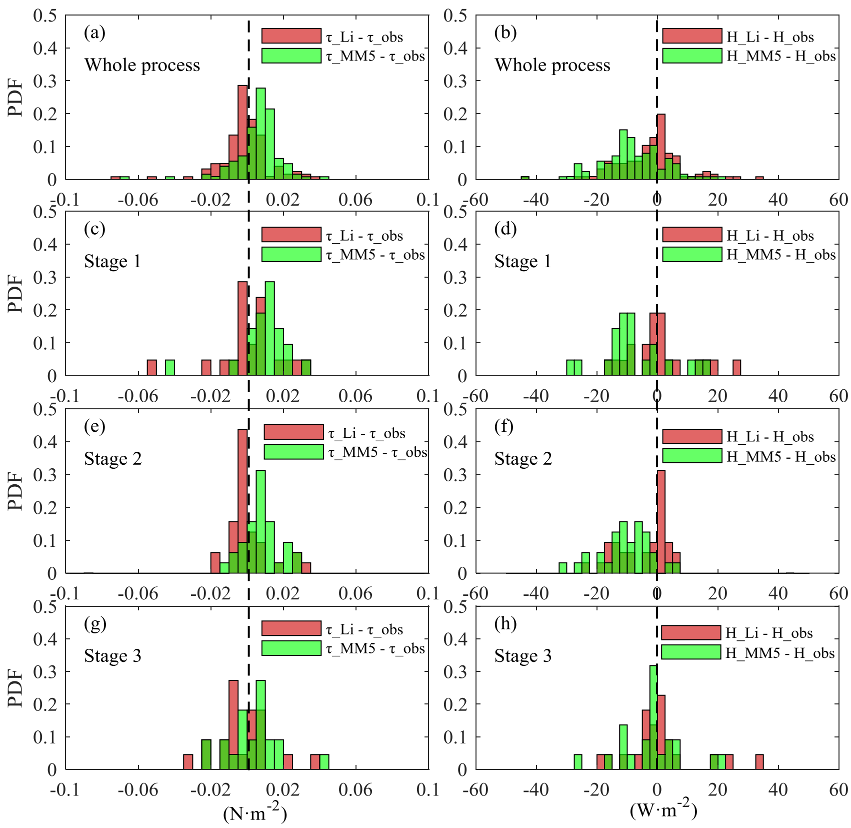

Figure 8. Probability distribution functions (PDF) of the difference between calculated fluxes (momentum fluxes: left; sensible heat fluxes: right) by using two schemes (the Li scheme: red bars; the MM5 scheme: green bars) and observations in different stages (a-b: whole process; c-d: stage 1; e-f: stage 2; g-h: stage 3).